Supporting Information

Belkhadir et al. 10.1073/pnas.1112840108

SI Experimental Procedures

Plant Cultivation, Ecotypes, and Mutants. The WT used in all experiments was *A. thaliana* accession Col-0. The *A. thaliana* accession Wassilewskija (Ws-0) was used as a control in Fig. 5. Plants were grown on soil or Petri dishes containing 0.5× Linsmaier and Skoog medium (Caisson Laboratories) in long-daylight conditions. For pathogen assays, plants were grown in growth chambers in short-day conditions. The following mutant plant genotypes were used in this work: *bak1-3* (1), *bri1* (GABI_134E10) (2), *fls2* (SALK_026801c), and *rpp4* (3). The insertion sites for the T-DNA lines (SALK_026801c) was located in the ORF of *FLS2*. Homozygosity of the *fls2* mutation and the sequence of the insertion site were confirmed by PCR and sequencing. The *fls2* mutant was confirmed to be a null allele by Western blot by using native anti-FLS2 polyclonal antibodies. The *sud1* allele has been described previously (4).

Transgenic Lines, Constructs, and Phenotypic Analysis. *BRI1*, *BAK1*, and *BKI1* tagged variant (mCitrine, mCherry, and HA tags) constructs were generated as described previously (2). Site-directed mutagenesis to generate the $BRI1^{sud1}$*mCitrine* allele was carried out following the site-directed mutagenesis protocol from Agilent Technology (formerly Stratagene), and the primers used are: sud1 forward (G643E), ACTAGCAGAGTCTATGAAGGTCACACTT C GCCG; and sud1 reverse (G643E), TGATCGTCTCAGATA CTTCCAGTGTGAAGCGGC. The constructs created and used are listed in Table S3. *BRI1* and *BAK1* constructs were transformed into WT Col-0, heterozygous *bri1* (2), and homozygous *bak1-3,* respectively, and their transgenic expression fully rescued the *bri1* and *bak1* dwarfism. For all constructs, more than 20 independent T1 lines were isolated and three to eight representative single insertion lines were selected in the T2 generation. Confocal microscopy, phenotypic analysis, and protein extraction were performed on segregating T2 and homozygous T3 lines as described previously (2). The functional *FLS2prom::FLS2::GFP* in Col-0 is a gift from Silke Robatzek (The Sainsbury Laboratory, Norwich, UK) (5). The *35S::DWF4* line in Col-0 was described previously (6). Table S2 includes a list and sources of transgenic lines used in this study.

Protein Analysis. Polyclonal anti-FLS2 antibodies were used at dilutions of 1:2,000 for immunodetection assays and 1:500 for immunoprecipitation (IP) assays. Antiphosphothreonine antibodies were used according to the manufacturer's instruction (Novagen). Protein extraction and quantification was performed as described previously (7); approximately 100 mg of 14-d-old light-grown seedlings were harvested for Western blot experiments. IP experiments were performed as described previously (8). Briefly, IP experiments required 1 g of seedlings (14 d old). Flash-frozen tissues were ground at 4 °C in a 15-mL tube containing 2 mL of ice-cold sucrose buffer [20 mM Tris, pH 8; 0.33 M sucrose; 1 mM EDTA, pH 8; protease inhibitor (Roche)] using a Polytron homogenizer (Brinkmann). Samples were centrifuged for 10 min at 5,000 × *g* at 4 °C or until the supernatants were clear. These total protein fractions were centrifuged at 4 °C for 45 min at 20,000 × *g* to pellet microsomes. The pellet was resuspended in 1 mL of IP buffer (20 mM Tris, pH 8, 0.33 M Sucrose, 150 mM NaCl, 0.5% Triton X-100) by using a 2-mL Potter–Elvehjem homogenizer.

Quantitative RT-PCR Analyses. Total RNA was isolated from frozen tissue (liquid nitrogen) by using the Spectrum Plant Total RNA Kit (cat. no. STRN250-1KT; Sigma) according to the manufacturer's instructions. One microgram of total RNA was added to each cDNA synthesis reaction using the First-Strand cDNA Synthesis Kit (cat. no. K1611; Fermentas). For quantitative real-time PCR, cDNA was synthesized, and DNA amplification was performed in the presence of SYBR Green qPCR Detection (Invitrogen) on the MyIQ Single Color Real-Time PCR Detection System (BioRad), using the following primer pairs: *WRK11* forward, ATGTCCAGCGAGGAAACACGT; reverse, TATTCTCCTGCATCGCGGATT; *WRKY6* forward, 5′-CAT ATTACCGCTGCACGATGG-3′; reverse, 5′-GGCAACGGATGGTTATGGTTT-3′; *WRKY29* forward, 5′-TTCGTTTTGCCTACCGATGG-3′; reverse, 5′-CGAGCTTGTGAGGATCGTTTG-3′; *WRK53* forward, 5′-AAATCCCGGCAGTGTTCCA-3′; reverse, 5′-TCTTGGCGATGATGACTCTCG-3′; *ACTIN 2/8* forward, 5′-TCTTGTTCCAGCCCTCGTTT-3′; reverse, 5′-TCTCGTGGATTCCAGCAGCT-3′; and *18S rRNA* forward, 5′-TATAGGACTCCGCTGGCACC-3′; reverse, 5′-CCCGGAACCCAAAAACTTTG-3′. The cycle used was: 95 °C for 1 min 30 s; 40× (95 °C for 10 s; 60 °C for 1 min); 95 °C for 1 min; 60 °C for 1 min and 81× (60 °C for 10 s). The relative mRNA levels were determined by normalizing the PCR threshold cycle number with actin and 18S rRNA. All experiments were repeated three times independently, and the average was calculated.

Pathogens and Cell Death Assays. *Pto* DC3000 and *hrc*C have been described previously (5). Bacterial growth in plant leaves was assessed by inoculating 4-wk-old plants with 10^5 cfu/mL. Growth inhibition of *Pto* DC3000 and *hrc*C by flg22 was conducted as described previously (8). Briefly, bacteria at a concentration of 10^5 cfu/mL were coinoculated with 1 μM flg22. For each sample, four leaf discs were pooled three times per data point (12 leaf discs total). Leaf discs were cored from the infiltrated area and ground to homogeneity in 10 mM $MgCl_2$, and the bacterial titer determined by serial dilution and plating. This experiment was repeated three times with consistent results. For *Hpa* sporangiophore growth assays, 12-d-old seedlings were inoculated with 32,000 spores/mL of the virulent *Hpa* isolate Noco2 or the avirulent isolate Emwa1. Plants were kept covered with a lid to increase humidity and grown at 20 °C with a 9-h light period. Sporangiophores were counted at 4 dpi (*Hpa* Noco2) or 5 dpi (*Hpa* Emwa1) by using a dissecting microscope (M205 FA; Leica). To evaluate infection in cotyledons, sporangiophores were counted on the adaxial and abaxial surfaces (9). Sporangiophores on primary leaves were counted only on the adaxial surface, as infected leaves often showed a strong epinastic phenotype. Trypan blue staining was performed to visualize cell death as described previously (4).

1. Jaillais Y, Belkhadir Y, Balsemão-Pires E, Dangl JL, Chory J (2011) Extracellular leucine-rich repeats as a platform for receptor/coreceptor complex formation. *Proc Natl Acad Sci USA* 108:8503–8507.
2. Jaillais Y, et al. (2011) Tyrosine phosphorylation controls brassinosteroid receptor activation by triggering membrane release of its kinase inhibitor. *Genes Dev* 25:232–237.
3. Knoth C, Ringler J, Dangl JL, Eulgem T (2007) Arabidopsis WRKY70 is required for full RPP4-mediated disease resistance and basal defense against Hyaloperonospora parasitica. *Mol Plant Microbe Interact* 20:120–128.
4. Hothorn M, et al. (2011) Structural basis of steroid hormone perception by the receptor kinase BRI1. *Nature* 474:467–471.
5. Robatzek S, Chinchilla D, Boller T (2006) Ligand-induced endocytosis of the pattern recognition receptor FLS2 in Arabidopsis. *Genes Dev* 20:537–542.
6. Lorrain S, Vailleau F, Balagué C, Roby D (2003) Lesion mimic mutants: Keys for deciphering cell death and defense pathways in plants? *Trends Plant Sci* 8:263–271.
7. Belkhadir Y, et al. (2010) Intragenic suppression of a trafficking-defective brassinosteroid receptor mutant in Arabidopsis. *Genetics* 185:1283–1296.
8. Belkhadir Y, Nimchuk Z, Hubert DA, Mackey D, Dangl JL (2004) Arabidopsis RIN4 negatively regulates disease resistance mediated by RPS2 and RPM1 downstream or independent of the NDR1 signal modulator and is not required for the virulence functions of bacterial type III effectors AvrRpt2 or AvrRpm1. *Plant Cell* 16:2822–2835.

9. Zipfel C, et al. (2004) Bacterial disease resistance in Arabidopsis through flagellin perception. *Nature* 428:764–767.

10. Symons GM, Reid JB (2004) Brassinosteroids do not undergo long-distance transport in pea. Implications for the regulation of endogenous brassinosteroid levels. *Plant Physiol* 135:2196–2206.

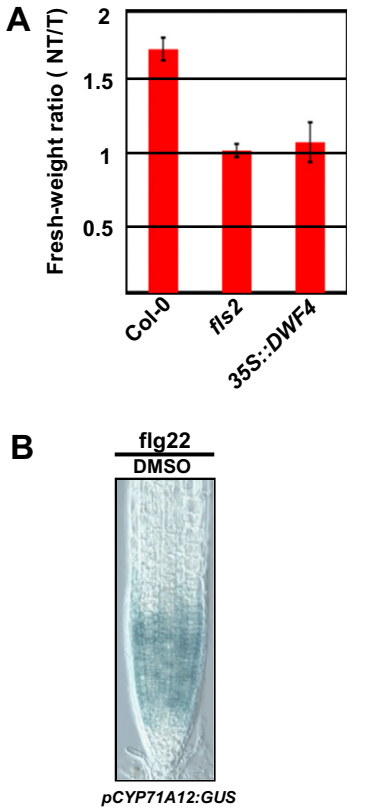

Fig. S1. Interplay between BR- and flg22-induced signaling. (*A*) Increased BR concentrations prevent flg22-induced growth inhibition. The red bar represents the average fresh-weight ratio of 14-d-old seedlings of the indicated genotypes grown for 7 d in water (NT) or 1 μM flg22 (T). Means and SDs were calculated from approximately 48 seedlings (six random pools of eight seedlings). This experiment was repeated three times with similar results. (*B*) Control GUS stain of the *CYP71A12::GUS* line. Seedlings were grown in the presence of DMSO the BRZ solvent and treated with 1 μM flg22 for 12 h before GUS staining.

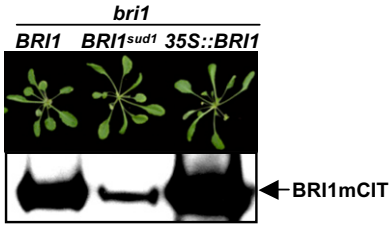

Fig. S2. Gain-of-function mutations in *BRI1* promote BR-independent cell elongation. Representative pictures of rosette stage transgenic *bri1* plants (T3) expressing *BRI1* or *BRI1*^{sud1} under the control of the native promoter or the CaMV35S promoter (*35S::BRI1*). The phenotypes associated with the overexpression of *BRI1* (*35S::BRI*)—narrow leaf blades and elongated and twisting petioles—were recapitulated by driving the expression of the BRI1^{sud1} variant under the control of the native promoter. *Bottom*: Microsomal protein extracts were prepared from *BRI1mCIT bri1*, *BRI1*^{sud1}*mCIT bri1*, and *35S::BRI1mCIT bri1* plants. These extracts were subjected to an anti-GFP protein immunoblot analysis to detect the accumulation of the mCitrine-tagged proteins. Equal loading was ensured by protein quantification before loading.

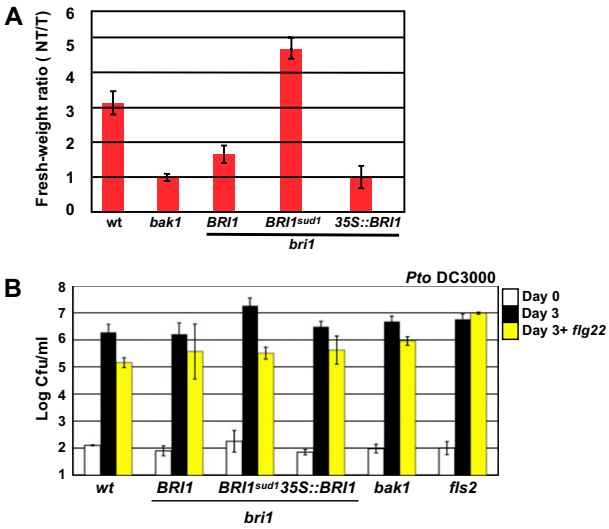

Fig. S3. BR signaling modulates responses to MAMPs. (*A*) The red bar represents the average fresh-weight ratio of 14-d-old seedlings of the genotypes indicated at the bottom grown for 7 d in water (NT) or 1 μM flg22 (T). Means and SDs were calculated from approximately 48 seedlings (six random pools of eight seedlings). This experiment was repeated three times with similar results. (*B*) Growth of *Pto*DC3000 was measured in the genetic backgrounds indicated at the bottom of the chart. Four-week-old plants were infiltrated with 10^5 cfu/mL *Pto*DC3000 in the presence (yellow bars) or absence (black bars) of 1 μM flg22. The number of bacteria per area of leaf was determined at 0 and 3 dpi. Values are mean cfu/mL; error bars represent ± 2 SE calculated from four internal replicate samples.

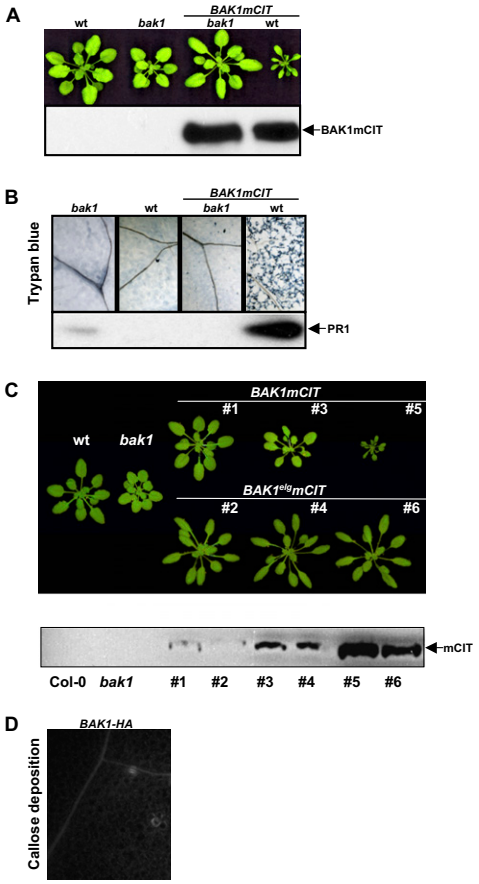

Fig. S4. Overexpression of *BAK1,* but not *BAK1*^{elg}, triggers inappropriate plant cell death. (*A*) *Top*: Images of representative rosettes of the genotypes listed. Functional complementation was confirmed by phenotypic rescue of the moderate dwarf phenotype of *bak1* in transgenic plants expressing *BAK1mCitrine* from the native promoter. *Bottom*: Microsomal protein extracts were prepared from the genotypes listed at the top. These extracts were subjected to anti-GFP immunoblot analysis to detect mCitrine-tagged proteins. Bradford protein quantification assay were used to confirm equal loading. (*B*) *Top*: Representative examples of 30 to 40 leaves of independent plants from each genotype listed at the top were trypan blue-stained and microscopically analyzed for cell death occurrence. *Bottom*: Total protein extracts were prepared from the genotypes listed at the top and subjected to anti-PR1 immunoblot. (*C*) *Top*: Images of representative rosettes of the genotypes listed in white expressing various levels of mCitrine-tagged *BAK1* (BAK1mCIT) and *BAK1*^{elg} (BAK1^{elg}mCIT) under the control of its native promoter. *Bottom*: Microsomal protein extracts were prepared from the genotypes listed in white and subjected to anti-GFP immunoblot analysis to detect mCitrine-tagged proteins. Plants expressing equivalent levels of BAK1 and BAK1^{elg} are matched from top to bottom (nos. 1 and 2, nos. 3 and 4, nos. 5 and 6). (*D*) Control aniline blue-stained callose deposits in the leaves of BAK1-HA plants treated with 1/2MS, but not flg22. This line was used for the cross with BRI1mCIT plants (Fig. 3*B*). Importantly, this *BAK1-HA* plant line does not display constitutive callose deposition.

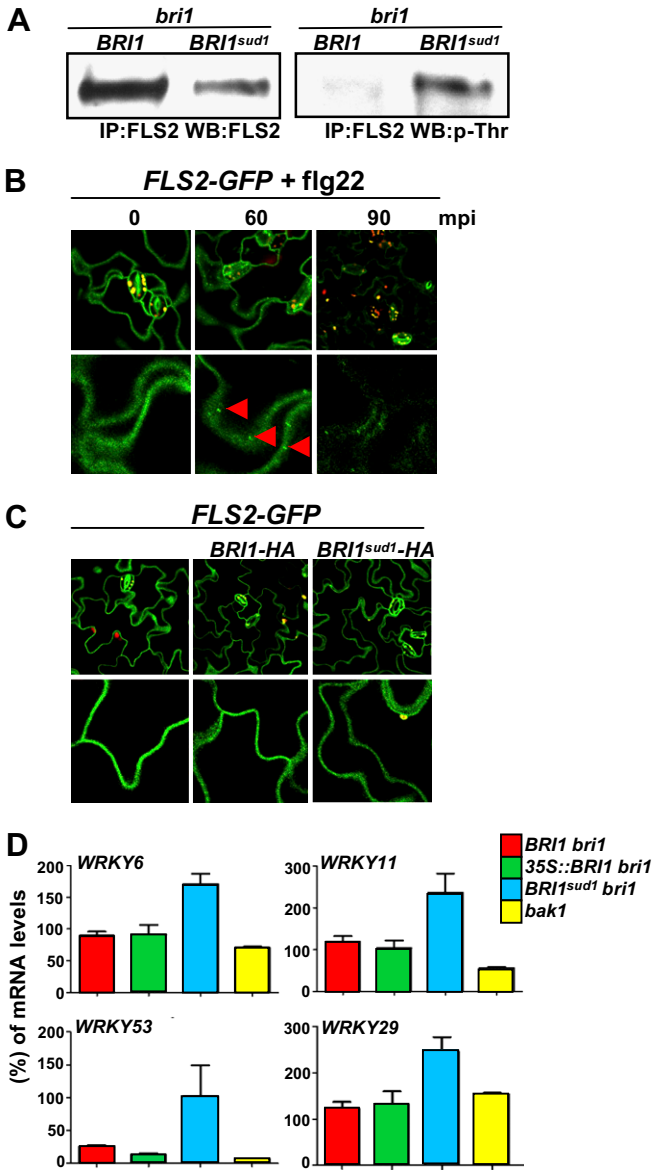

Fig. S5. *BRI1*^{sud1} affects FLS2 activation state and basal defenses gene expression. (*A*) Microsomal protein extracts prepared from *BRI1* and *BRI1*^{sud1}*mCIT* seedlings were immunoprecipitated with anti-FLS2 antibody (IP; FLS2) and analyzed with anti-FLS2 antibody (WB; FLS2) or antiphosphothreonine antibody (WB; p-Thr). (*B*) Intracellular dynamics of FLS2-GFP in response to flg22. Two-week-old FLS2-GFP seedlings were treated with a solution of 10 μM flg22. GFP signal was monitored over a period of 90 min by confocal microscopy of leaf epidermal cells. Red arrows show the appearance of nascent endosomes. Our results confirm previously published results demonstrating that FLS2 is internalized and disappears upon flg22 treatment (5). (*C*) *FLS2-GFP BRI1-HA* or *FLS2-GFP BRI1*^{sud1}*-HA* double transgenic lines were constructed by crossing an FLS2-GFP line to homozygous T2 plants transformed with an HA epitope-tagged *BRI1* transgene driven by the native promoter. FLS2 localization and internalization state was monitored in the absence of flg22. Our results indicate that the steady-state distribution of FLS2 intracellular pools is not modified in *BRI1*^{sud1} plants. (*D*) Quantitative real-time PCR analyses of the indicated *WRYK* transcripts from seedlings of the genotypes listed on the right.

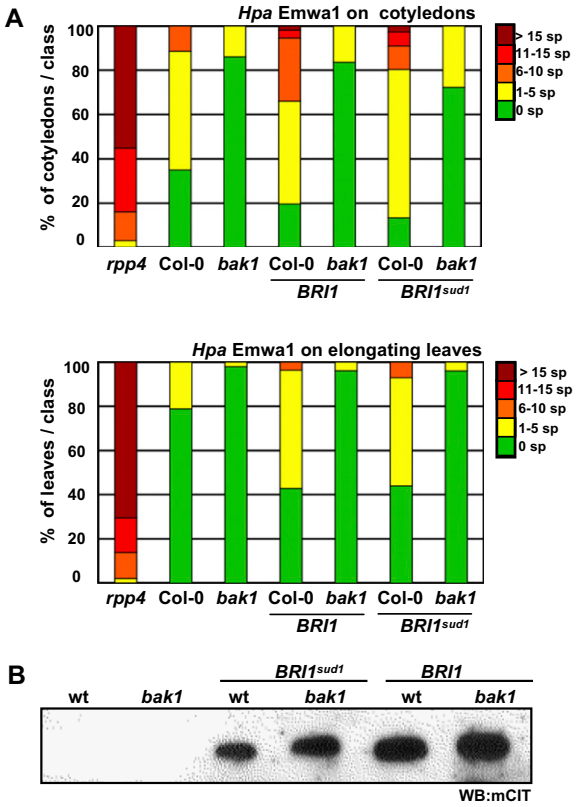

Fig. S6. Enhanced BR signaling affects RPP4-mediated resistance in a BAK1-dependent manner. (*A*) Twelve-day-old cotyledons of the genetic backgrounds indicated at the bottom of the chart were inoculated with conidiospores of the avirulent *Hpa* isolate Emwa1 at 32,000 spores/mL. Sporangiophores were counted 5 d after inoculation on cotyledons (*Upper*) and first true leaves (*Lower*) for each of the indicated genetic backgrounds. Means, sample size, and 2 × SE are presented in Table S1. Note that the T2 *BRI1mCitrine* (*BRI1*) or *BRI1*^{sud1}*mCitrine* (*BRI1*^{sud1}) plants express *BRI1* under the control of the native promoter in the WT (Col-0) or *bak1* genetic backgrounds. sp, sporangiophores per cotyledon (*Top*) or sporangiophores per leaf (*Bottom*). (*B*) Microsomal protein extracts were prepared from the genotypes listed at the top. These extracts were subjected to an anti-GFP protein immunoblot analysis to detect the accumulation of the mCitrine-tagged proteins (*Bottom*). Equal loading was ensured by protein quantification before loading.

Table S1. Raw data from *Hpa* assays

	Hpa Noco2 32,000 spores/mL 4 dpi						*Hpa* Emwa1 32,000 spores/mL 5 dpi					
	Cotyledons			Primary leaves			Cotyledons			Primary leaves		
	With sporangiophores, %	Mean ± 2 SE	Sample size*	With sporangiophores, %	Mean ± 2 SE	Sample size*	With sporangiophores, %	Mean ± 2 SE	Sample size*	With sporangiophores, %	Mean ± 2 SE	Sample size*
Ws	0.0	0.0 ± 0.0	81	0.0	0.0 ± 0.0	40	ND	ND	ND	ND	ND	ND
rpp4	ND	ND	ND	ND	ND	ND	100.0	15.9 ± 0.5	100	100.0	17.3 ± 0.7	51
Col-0	80.2	8.2 ± 0.7	101	88.9	9.3 ± 0.9	72	64.9	2.2 ± 0.2	114	21.1	0.2 ± 0.1	57
bak1	60.9	5.0 ± 0.7	92	65.0	4.6 ± 0.7	60	13.9	0.2 ± 0.1	115	2.0	0.0 ± 0.0	51
BRI1	86.7	11.5 ± 0.8	105	98.1	16.6 ± 0.8	52	80.4	4.2 ± 0.4	112	57.1	1.3 ± 0.2	56
BRI1 bak1	40.2	1.5 ± 0.3	97	38.5	2.9 ± 0.7	52	16.3	0.2 ± 0.0	104	5.8	0.0 ± 0.0	53
BRI1 ^{sud1}	88.2	11.1 ± 0.8	102	92.6	14.6 ± 1.0	54	86.6	3.8 ± 0.4	112	56.1	1.4 ± 0.3	57
BRI1 ^{sud1} *bak1*	42.1	2.5 ± 0.5	95	49.0	3.0 ± 0.6	51	27.7	0.4 ± 0.1	101	5.9	0.0 ± 0.0	51

ND, not detected.

*No. of cotyledons or primary leaves.

Table S2. Transgenic lines tested in this study

Transgenic line	Promoter	Epitope tag/gene fusion	Genetic background	Ref.
35S::DWF4	35S CaMV	None	Col-0	1
pCYP71A12::GUS	*CYP71A12* native promoter	GUS	Col-0	2
BRI1	BRI1 native promoter	mCitrine	Col-0	3
BRI1 bri1	BRI1 native promoter	mCitrine	*bri1* T-DNA null	3
BRI1 bak1	BRI1 native promoter	mCitrine	bak1-3 null	Present study
BRI1sud1	BRI1 native promoter	mCitrine	Col-0	Present study
BRI1sud1 bri1	BRI1 native promoter	mCitrine	*bri1*T-DNA null	Present study
BRI1sud1 bak1	BRI1 native promoter	mCitrine	bak1-3	Present study
BRI1-HA	BRI1 native promoter	HA	Col-0	3
BRI1sud1-HA	BRI1 native promoter	HA	Col-1	Present study
35S::BRI1 bri1	35S CaMV	mCitrine	*bri1* T-DNA null	Present study
BAK1-HA	BAK1 native promoter	HA	Col-0	Present study
BAK1mCIT	BAK1 native promoter	mCitrine	Col-0	3, 4
BAK1mCIT bak1	BAK1 native promoter	mCitrine	bak1-3 null	4
BAK1mCHE	BAK1 native promoter	mCherry	Col-0	3
BKI1mCIT	UBIQUITIN promoter	mCitrine	Col-0	3
FLS2-GFP	FLS2 native promoter	GFP	Col-0	5

1. Nemhauser JL, Mockler TC, Chory J (2004) Interdependency of brassinosteroid and auxin signaling in Arabidopsis. *PLoS Biol* 2:E258.
2. Millet YA, et al. (2010) Innate immune responses activated in Arabidopsis roots by microbe-associated molecular patterns. *Plant Cell* 22:973–990.
3. Jaillais Y, et al. (2011) Tyrosine phosphorylation controls brassinosteroid receptor activation by triggering membrane release of its kinase inhibitor. *Genes Dev* 25:232–237.
4. Jaillais Y, Belkhadir Y, Balsemão-Pires E, Dangl JL, Chory J (2011) Extracellular leucine-rich repeats as a platform for receptor/coreceptor complex formation. *Proc Natl Acad Sci USA* 108: 8503–8507.
5. Robatzek S, Chinchilla D, Boller T (2006) Ligand-induced endocytosis of the pattern recognition receptor FLS2 in Arabidopsis. *Genes Dev* 20:537–542.

Table S3. Plasmid constructs used in this study

Construct name	Binary vector	Resistance in plant
BAK1prom::BAK1-mCITRINE (BAK1-CITRINE)	*pB7m34GW*	Basta
BAK1prom::BAK1-mCHERRY (BAK1-CHERRY)	*pH7m34GW*	Hygromycin
BAK1prom::BAK1-6xHA (BAK1-6xHA)	*pK7m34GW*	Kanamycin
35Sprom::BRI1-CITRINE (OxBRI1-CITRINE)	*pB7m34GW*	Basta
BRI1prom::BRI1-mCITRINE (BRI1-mCITIRINE)	*pB7m34GW*	Basta
BRI1prom::BRI1-6xHA (BRI1-6xHA)	*pK7m34GW*	Kanamycin
BRI1prom::BRI1sud1-mCITRINE (BRI1sud1-mCITRINE)	*pB7m34GW*	Basta
BRI1prom::BRI1sud1-6xHA (BRI1sud1-6xHA)	*pK7m34GW*	Kanamycin
UBQ10prom::BKI1-mCITRINE (BKI1-mCITRINE)	*pB7m34GW*	Basta

Further details are provided in Jaillais et al. (1).

1. Jaillais Y, et al. (2011) Tyrosine phosphorylation controls brassinosteroid receptor activation by triggering membrane release of its kinase inhibitor. *Genes Dev* 25:232–237.